Microstructure and formation mechanism of Ce-based chemical conversion coating on 6063 Al alloy

CHEN Dong-chu(陈东初)[1,2], LI Wen-fang(李文芳)[1], GONG Wei-hui(龚伟慧)[1],
WU Gui-xiang(吴桂香)[1], WU Jian-feng(吴建峰)[2]

1. School of Materials Science and Engineering, South China University of Technology,
Guangzhou 510640, China;
2. School of Science, Foshan University, Foshan 528000, China

Abstract: In order to accelerate the conversion coating formation on 6063 Al alloy in the $Ce(NO_3)_3$ solution, accelerants of chloride and ammonium salt were used. The coating morphology, composition and structure were analyzed with SEM/EDS, EPMA, XPS and XRD. The coating morphology is influenced by the composition, pH value and temperature of the treating solution. The coating composed of metal oxide, metal hydroxide and hydrate appears to be amorphous. The elements in the coating are Al, Ce, O, Mn and Mg, while the Ce element exists in the forms of Ce^{3+} and Ce^{4+}. The accelerant of chloride can increase the compactness and Ce content of the coating, so the coating corrosion resistance is remarkably improved. A scheme for the electrochemical reaction in the coating formation was proposed, and the potential change in the coating formation was also studied. It is found that chloride can shorten the time period of the first and the second stages in coating formation.
Key words: aluminum alloy; conversion coating; rare-earth element

1 Introduction

In order to reduce the tendency towards corrosion and improve the adhesion with the paint, the aluminium alloy surface is typically modified by a chromate-based chemical conversion pretreatment. Despite the undeniable qualities and advantages of this chromate treatment, such technology should be soon withdrawn from any industrial process since hexavalent chromium has been recognized to be highly toxic and carcinogenic [1−2]. Currently, much effort was made to develop more benign alternatives. Among the various reported alternatives, such as treatments with fluotitanic or fluozirconic acid, cobalt salt, and phosphate permanganate[3−6], rare earth elements based treatment was believed as one of the most promising systems, and many researchers have reported many treating solutions with rare earth salts (cerium, lanthanum, neodymium and yttrium) which could effectively inhibit the corrosion of aluminum alloys[7−10]. Although much progress has been made in the processes with cerium salts, up to now, the efficiency of these developed treating methods is not really equal to that of the traditional chromate treatment, and long time-duration or high temperature is needed in these processes[11]. In addition, so far there is few report about the effect of the additives upon the coating growth[12]. In this work, a $Ce(NO_3)_3$ based treating solution was adopted, and chloride and ammonium salts were used to accelerate the coating formation. SEM/EDS, EPMA, XPS, XRD were used to observe the coating morphology or analyze the coating structure and composition. In order to study the coating formation mechanism, a scheme for the electrochemical reaction on the 6063 Al alloy surface was presented, and the potential change in the coating growth of the Al alloy in different solutions was also analyzed.

2 Experimental

Rectangular specimens (6063 Al alloy) were in the size of 20 mm×20 mm×3 mm. The surface of the

specimens was firstly mechanically polished by 200, 600 and 1000 grit emery papers. After the pretreatment of degreasing, alkaline deoxidization and acid polishing to remove the surface contamination, the specimens were treated in chemical conversion bath. Finally, they were rinsed with distilled water and dried with cool air.

The chemical conversion treatment solution mainly comprised of $Ce(NO_3)_3$ and $KMnO_4$. $L_{16}(4^3)$ orthogonal experiment was carried out to optimize the electrolyte composition. The pH value was adjusted with 0.1 mol/L NaOH or 0.1 mol/L HNO_3 to study the effect of solution pH value on the coating formation. Accelerants of chloride and ammonium salt were added to the optimal treating solution, then the effect of accelerants on the coating growth was studied. The coating thickness was measured with eddy current thickness tester (Surfix-FNB).

SEM (scanning electron microscopy), EDX (energy dispersive X-ray spectroscopy), EPMA (electron probe X-ray microanalysis), XRD (X-ray diffraction) and XPS (X-ray photoelectron spectroscopy) were used to observe the morphology and structure as well as to identify the element compositions of the chemical conversion coating.

The corrosion resistance of the formed coating was evaluated by potentiodynamic polarization curve determined in 3.5% NaCl solution, and the potential change (φ—t curve) of the Al alloy in the treating solution was recorded with an electrochemistry station (AUTOLAB PGSTAT30, Switzerland).

3 Results and discussion

3.1 Micro-morphology of conversion coating

Fig.1 shows the SEM images of the specimens treated in the different conditions. In the solution of 5 g/L

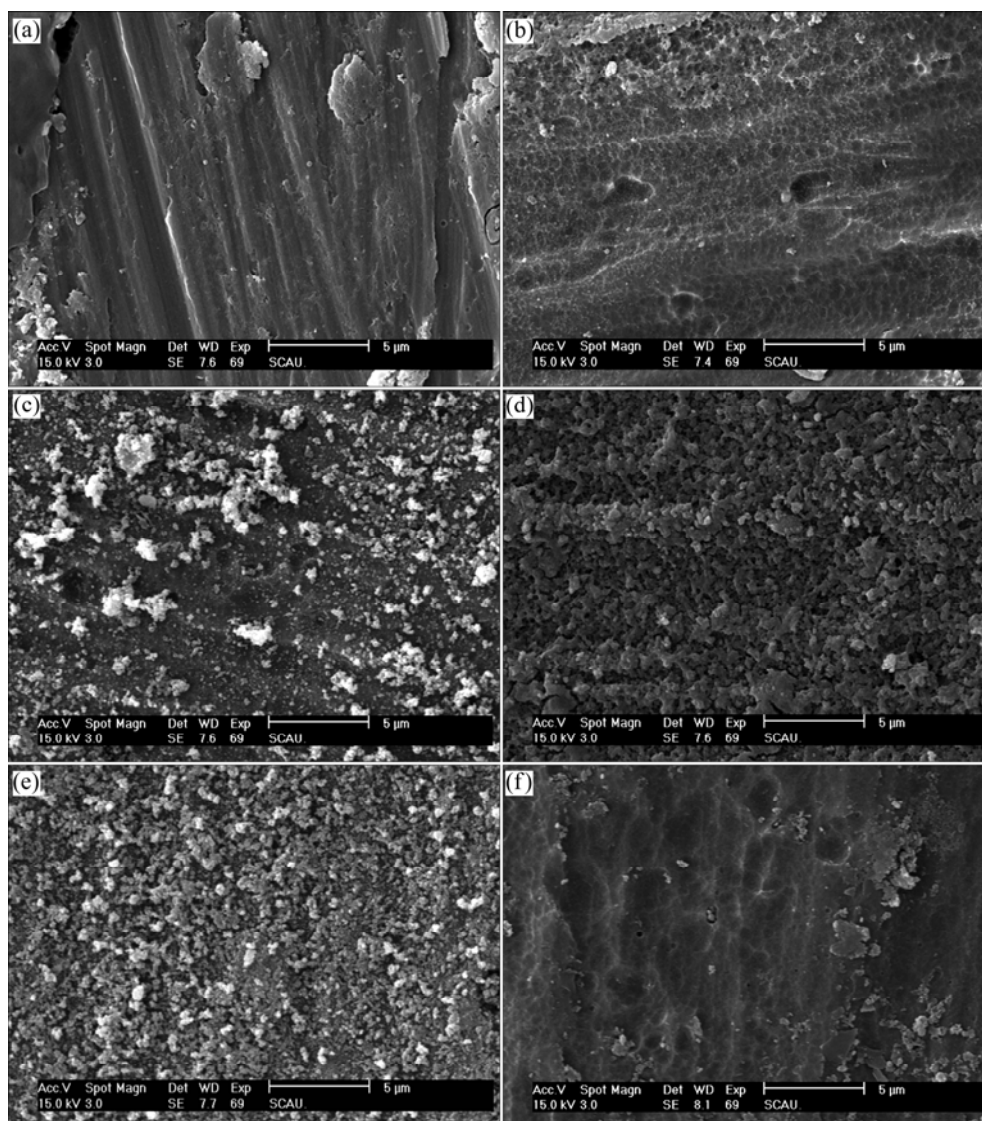**Fig.1** Effect of treating process on coating surface morphology: (a) 5 g/L $Ce(NO_3)_3$, 1 g/L $KMnO_4$, 20 ℃; (b) 5 g/L $Ce(NO_3)_3$, 2 g/L $KMnO_4$, 40 ℃; (c) 20 g/L $Ce(NO_3)_3$, 3 g/L $KMnO_4$, 40 ℃; (d) 10 g/L $Ce(NO_3)_3$, 4 g/L $KMnO_4$, 60 ℃; (e) 10 g/L $Ce(NO_3)_3$, 3 g/L $KMnO_4$, 80 ℃; (f) 15 g/L $Ce(NO_3)_3$, 2 g/L $KMnO_4$, 80 ℃

$Ce(NO_3)_3$ and 1 g/L $KMnO_4$ at 20 ℃, the coating grows very slowly, which is too thin to cover the polishing trace on Al matrix. The elevated temperature will accelerate the coating growth, as shown in Fig.1(b) formed at 40℃. The specimen treated in solution of 10 g/L $Ce(NO_3)_3$ and 4 g/L $KMnO_4$ at 60 ℃ has the best coating quality (Fig.1(d)), but the quick deposition of oxide at the high concentration of 20 g/L $Ce(NO_3)_3$ or at the high solution temperature of 80 ℃ will worsen the coating compactness, as shown Figs.1(c) and (f), of which the coating is loose and coarse. Therefore, it is necessary to control the solution concentration of $Ce(NO_3)_3$ less than 10 g/L and solution temperature less than 60 ℃ to produce a good conversion coating on Al alloy surface.

　　The pH value of the treating solution was adjusted with NaOH and HNO_3, and the SEM photographs of the coating formed in the solutions of different pH values are shown in Fig.2. The compactness of conversion coatings is gradually decreased and they are easy to break off when the solution pH value exceeds 1.0. The coating reaches its maximal thickness of 7.6 μm when treated in pH 1.9 solution. Too much OH^- in the solution dramatically accelerates the deposition of $Ce(OH)_3$ and $Ce(OH)_4$, as a result, the conversion coatings formed in the solutions of pH＞1.0 are loose and vulnerable to come off, which will worsen the corrosion resistance of the coating.

　　Figs.3(a) and (b) show the SEM images of the coating treated in the solution containing 1.6 g/L chloride and 0.4 g/L ammonium salt, respectively, from which it can be seen that the coating formed in the treating solution with chloride is very compact and even; but when treated in the bath with ammonium salt, the coating is covered by many loose particles, which worsens the coating compactness and adhesion on the Al matrix.
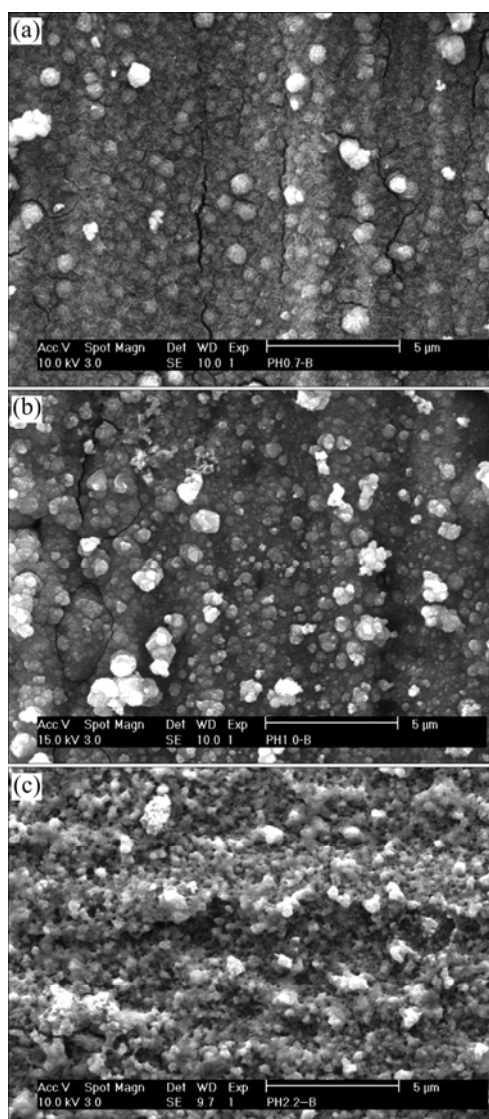
Fig.2 Effect of solution pH value on coating surface morphology: (a) pH 0.7; (b) pH 1.0; (c) pH 2.2
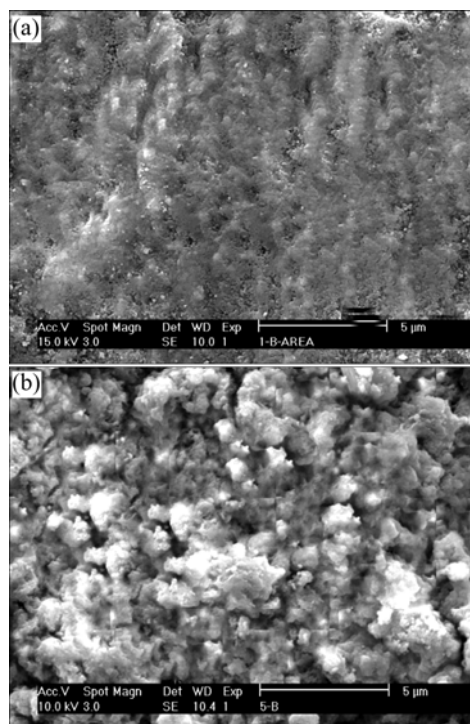
Fig.3 Coating micro-morphologies formed with accelerants: (a) Chloride; (b) Ammonium salt

　　Chloride is superior to ammonium salt in the coating anti-corrosion performance improvement, as seen in the polarization curves of Fig.4. The J_{corr} of Al matrix and the specimens treated in the solutions without accelerant and with accelerants of 0.4 g/L ammonium salt and 1.6 g/L chloride are 6.78×10^{-6}, 0.84×10^{-6}, 0.32×10^{-6}, $0.15 \times 10^{-6} A/cm^2$, respectively.

　　The corrosion resistance of the specimen treated in the solution with 0.4 g/L ammonium salt, which accelerates the coating growth and increases the coating

Fig.4 Polarization curves of specimens treated in different conditions

thickness from 2.9 μm to 4.6 μm, can be increased by 0.6 times as compared with that of the specimen treated in the solution without accelerant. The maximal corrosion resistance of the specimen obtained in the solution with the addition of 1.6 g/L chloride is 4.6 times higher than the specimen treated in the solution without accelerant.

3.2 Elemental composition and elemental cross-distribution in conversion coating

EDX was used to analyze the element composition in the coating treated in the different conditions, as listed in Table 1. All the coating formed in the different solutions have the same elemental composition, but the accelerants change the element content in the coating. Chloride increases the Ce content in th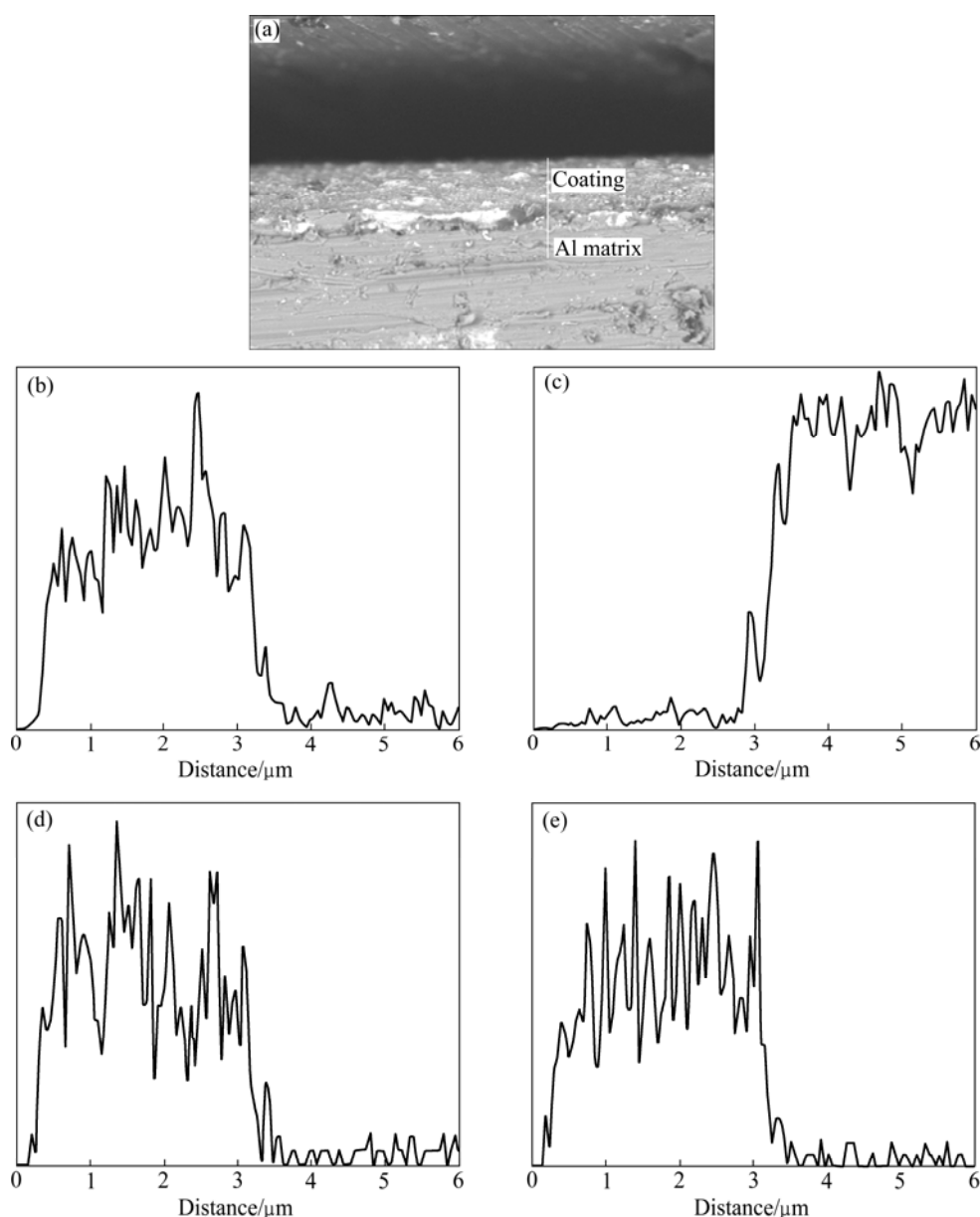e coating, while ammonium salt decreases it, leading to the evolution of Al content, so it can be known that the accelerants can facilitate the deposition of Ce or Al hydroxides.

The Ce content in the coating is also influenced by the pH value in the treating solution, as seen in Table 2. The molar fraction of Ce rises from 0.485% to 5.93% with the pH value increasing from 0.7 to 1.9, because the high concentration of OH^- in the solution dramatically accelerates the deposition of $Ce(OH)_3$ and $Ce(OH)_4$. But

the too quick coating growth worsens the coating compactness and leads to the coating coming off easily, as seen in Fig.2, so the Ce content decreases from 5.93% to 3.695% (molar fraction) when the pH value rises from 1.9 to 2.2.

Fig.5 shows the elements distribution along the cross-section direction of the coating with EPMA analysis, from which it can be seen that the conversion coating is mainly composed of Ce, Al, Mn and O, and the elements of Ce, Al, Mn and O almost distribute homogeneously in the cross-section direction of the coating. It is also known that not only the components in the solution but also Al matrix take part in the coating formation.

3.3 Element composition and valence of conversion coating

Fig.6 shows the XPS spectra for the conversion coating. The coating is mainly composed of Al, Mn, Ce and O, extremely corresponding to the EPMA result in Fig.5. Figs.6(b), (c) and (d) show the XPS spectra for the single element of Mn, Ce and O respectively. Fig.6(c) shows the overlap of the Ce peaks of different valences, so it can be known that the Ce element probably exists in the forms of Ce^{3+} and Ce^{4+}. Seen in Fig.6(d), the signal of O 1s can be attributed to the lattice oxide ions O^{2-}, to OH^- group and to strongly bound water H_2O. It can be concluded that the coating is mainly composed of metal oxides, metal hydroxides and its hydrates, and the Ce oxide probably exists in the forms of Ce_2O_3, CeO_2, $Ce(OH)_3$, $Ce(OH)_4$ and their hydrates.

3.4 Microstructure of conversion coating

Fig.7 shows the XRD patterns of the coating formed on 6063 Al alloy. These four intense diffraction peaks from 38° to 85° are attributed to the Al matrix. The appearance of the bread-shaped peak from 20° to 36° in the XRD pattern indicates that the deposited coating on the Al surface is in the amorphous structure. The intensity of the bread-shaped peak is strengthened when accelerant of chloride is added to the treating bath, while accelerant of ammonium salt makes little devotion to the increment of diffraction peak intensity. From the XRD

Table 1 Composition of coating treated in different solutions

Element	No accelerant		With chloride accelerant		With ammonium salt accelerant	
	w/%	x/%	w/%	x/%	w/%	x/%
O L	28.43	56.83	26.28	54.62	20.23	41.36
Al K	6.95	8.24	5.56	6.86	25.62	31.07
Ce L	25.99	5.93	39.06	9.27	17.82	4.15
Mn K	32.10	16.68	22.78	13.79	19.77	11.77
Others	Bal.	Bal.	Bal.	Bal.	Bal.	Bal.

Fig.5 EPMA results of element distribution along cross-section direction of coating: (a) Morphology; (b) Distribution of O element; (c) Distribution of Al element; (d) Distribution of Ce element; (e) Distribution of Mn element

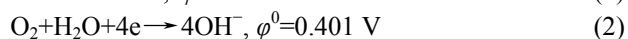**Table 2** Ce content in conversion coating treated in solution of different pH values

pH value	w/%	x/%
0.7	2.522	0.485
1.3	5.719	1.173
1.9	25.990	5.930
2.2	16.988	3.695

pattern, it is also known that the addition of accelerants do not lead to the formation of new structure.

3.5 Coating formation mechanism
3.5.1 Electrochemical reaction in coating formation

6063 Al alloy is a type of Al-Mg-Si alloy, and its surface is of chemical heterogeneity. The negative potential phase acts as an active anode, while the positive potential phase acts as an active cathode in the treating solution[8]. The electrochemical reaction for coating formation on aluminium alloy surface can be described in Fig.8, where Al dissolves in the micro-anode area, and oxygen and oxidant are reduced in the micro-cathode area:

$$Al-3e \longrightarrow Al^{3+}, \quad \varphi^0 = -1.67 \text{ V} \qquad (1)$$
$$O_2+H_2O+4e \longrightarrow 4OH^-, \quad \varphi^0 = 0.401 \text{ V} \qquad (2)$$

or in the acid solution:

$$O_2+4H^++4e \longrightarrow H_2O, \quad \varphi^0 = 1.229 \text{ V} \qquad (3)$$
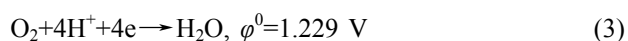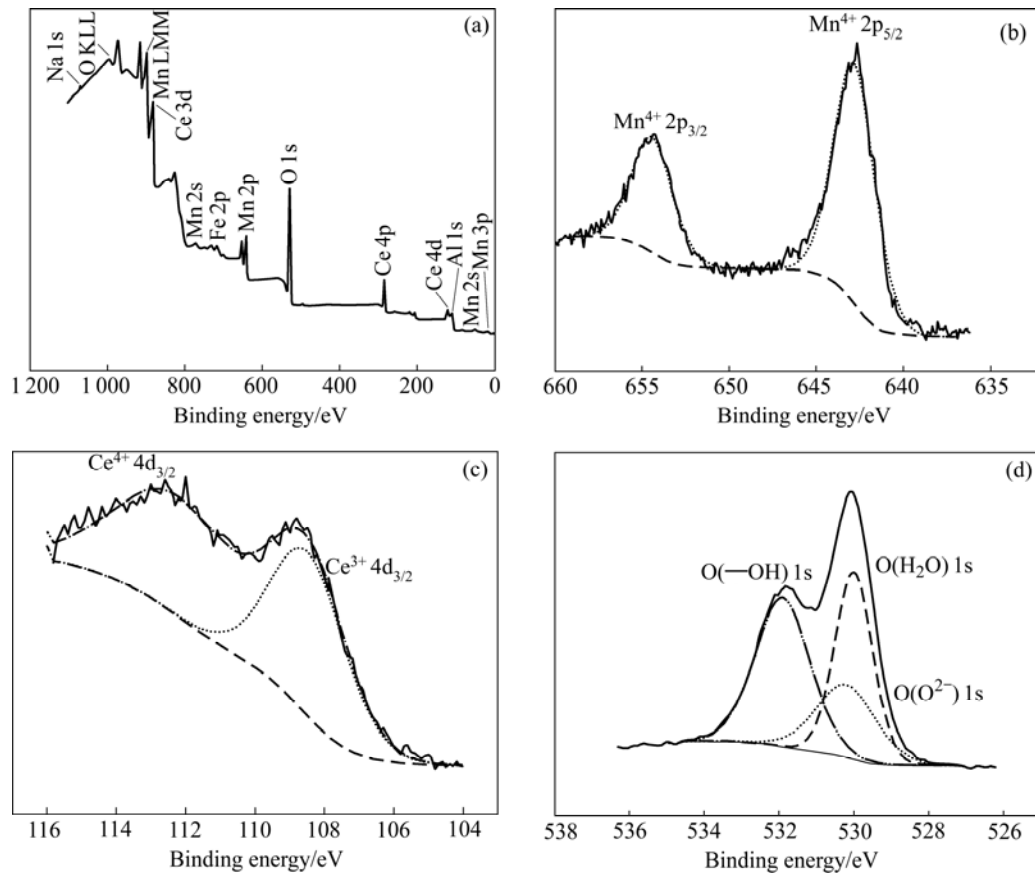
Fig.6 XPS spectra for conversion coating surface: (a) All elements; (b) Mn; (c) Ce; (d) O
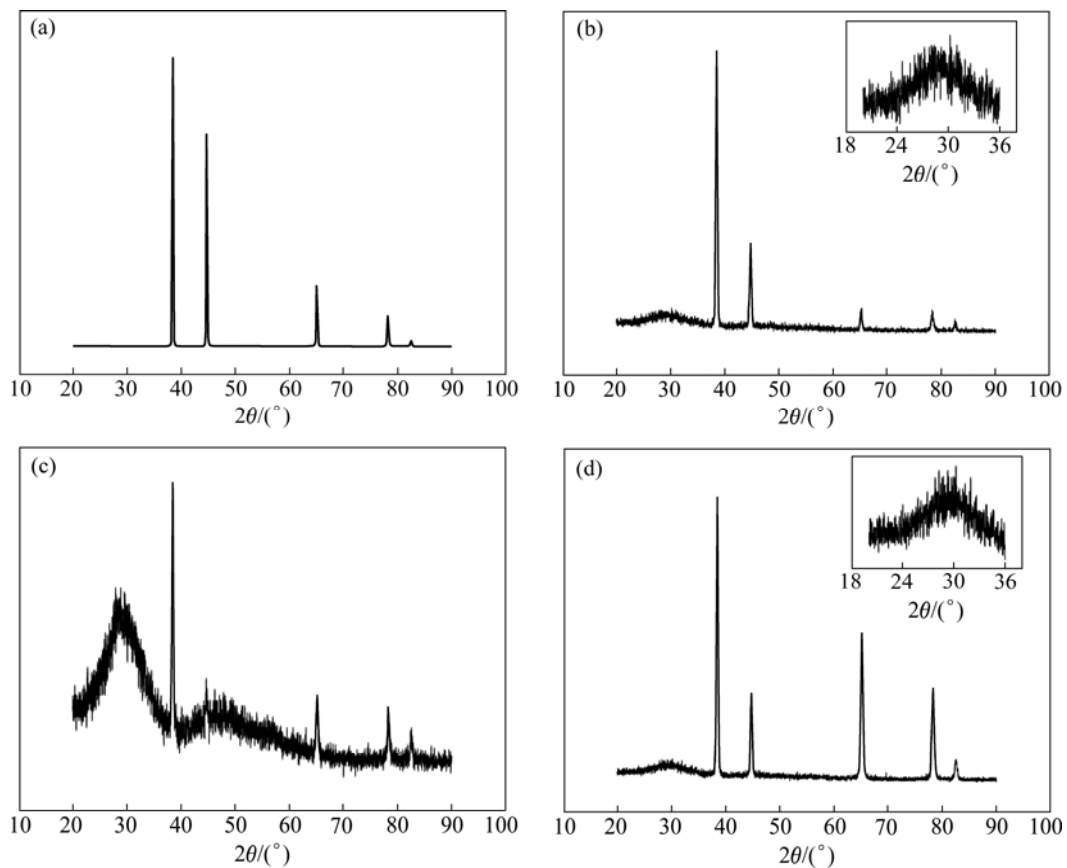
Fig.7 XRD patterns of chemical conversion coating treated in different solutions: (a) Al matrix; (b) No accelerant; (c) With accelerant of chloride; (d) With accelerant of ammonium salt
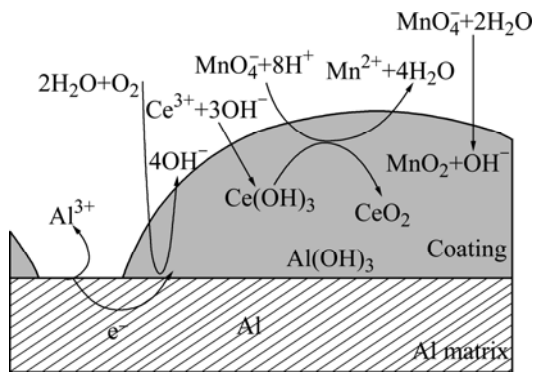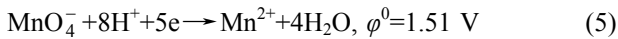
Fig.8 Scheme for electrochemical reaction of coating formation on aluminium alloy surface

The dissolved Al^{3+} can be deposited as

$$Al^{3+}+3OH^- \longrightarrow Al(OH)_3 \downarrow \qquad (4)$$

The added oxidant of $KMnO_4$ will accelerate the cathodic reaction, and the reaction is written as[13]

$$MnO_4^- +8H^+ +5e \longrightarrow Mn^{2+}+4H_2O, \ \varphi^0=1.51 \ V \qquad (5)$$

As the pH around the micro-cathode sites increases to a critical value for $Ce(OH)_3$ formation, Ce^{3+} will deposit on the micro-cathode surrounding[14]:

$$Ce^{3+}+3H_2O \longrightarrow Ce(OH)_3 \downarrow +3H^+ \qquad (6)$$

or written as

$$Ce^{3+}+3OH^- \longrightarrow Ce(OH)_3 \downarrow$$
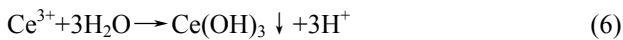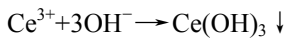
The critical pH can be calculated by:

$$pH_c=1/3(22.15-lg[Ce^{3+}]) \qquad (7)$$

Putting 0.031 mol/L of $[Ce^{3+}]$ into Eq.(7), the pH_c value is 7.88, lower than that (pH=10.65, calculated by the HÖHM et al[15]) around the micro-cathode areas. Therefore, $Ce(OH)_3$ prefers to deposit at cathodic sites, and its size gradually grows from the firstly formed nucleus to particles on the surface. Fig.9 shows the EDX spectra of the conversion coating surface. It is indicated that the Ce content in the particles (Fig.2) is 10.249% (molar fraction), which is higher than the average value of that in the whole coating, i.e., 5.93%.

The potential of Eq.(5) can be written as $\varphi^0=1.51+0.094pH$, and its value at the micro-cathode, where the pH is 10.65, is 2.51 V. The deposited $Ce(OH)_3$ can be oxidized by $KMnO_4$ to CeO_2 through the following reaction:

$$Ce(OH)_3+H_2O \longrightarrow CeO_2+H^++e, \ \varphi^0=1.559-0.059pH \quad (8)$$
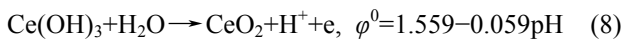
$\varphi^0(Ce^{4+}/Ce^{3+})$, the potential on the micro-cathode (pH=10.65) is about 0.93 V, so Ce^{3+} can be oxidized to Ce^{4+}, and that is why the valences of Ce element in coating are +3 and +4.
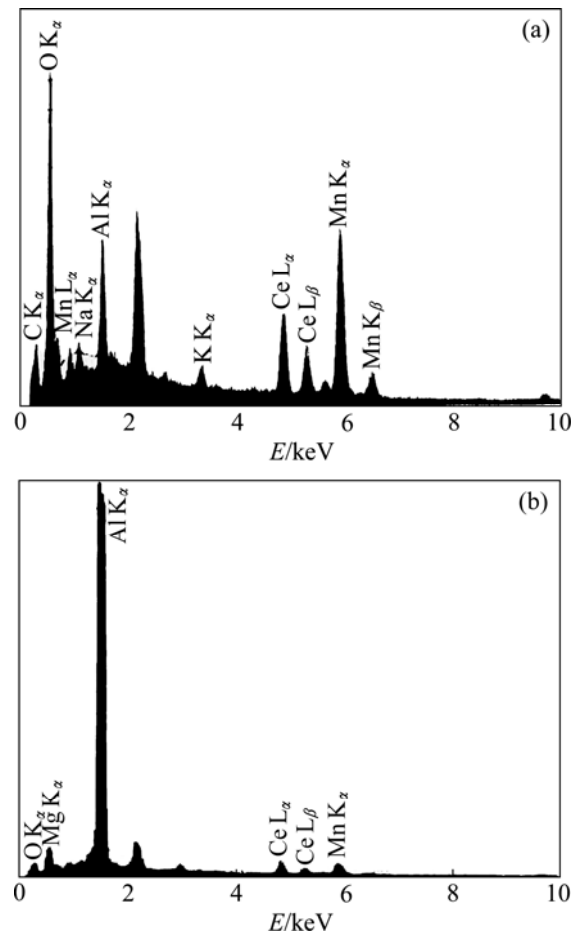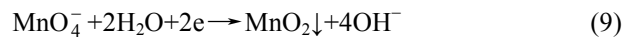

Fig.9 EDX spectra for different sites on coating surface: (a) For particle; (b) For particle surrounding

As the above reaction proceeds, they lead to the local rising of $[OH^-]$ on the surface of micro-cathode, and another reaction will occur in the solution of low H^+ concentration[13]:

$$MnO_4^- +2H_2O+2e \longrightarrow MnO_2 \downarrow +4OH^- \qquad (9)$$

3.5.2 Potential change in coating formation process

The potential change of the specimen in the coating growth process was recorded with an electrochemical measuring system, and the $\varphi—t$ curves are shown in Fig.10. Fig.10(a) indicates the $\varphi—t$ curve in the coating growth process can be divided into three stages[16]. The first stage is in period less than 6 min, in which the potential quickly increases for the dissolution of Al alloy and the accumulation of the dissolved Al^{3+} in the interface between Al matrix and solution[16]. The conversion coating begins to form gradually in this stage, shown as the reactions of Eqs.(4−5). In the second stage, the potential change is really slow when the Al dissolution is blocked by the formed coating, and the deposition of $Ce(OH)_3$ or CeO_2 will reach a balance as

Eqs.(6) and (8). The local [OH$^-$] in micro-cathode area will rise after the first and second stage, and new reaction of Eqn.(10) will occur in the third stage[13]. MnO$_2$ or its hydrate H$_2$MnO$_3$ will co-deposit with the metal oxides or metal hydroxides (Ce(OH)$_3$, CeO$_2$, Al(OH)$_3$) on the surface, so the thickness of the coating will further increase in the third stage.

Fig.10(b) shows the $\varphi-t$ curves recorded in different solutions for the specimen in coating formation process, from which it is known that the initial potentials of Al alloy all move positively when accelerants are added.
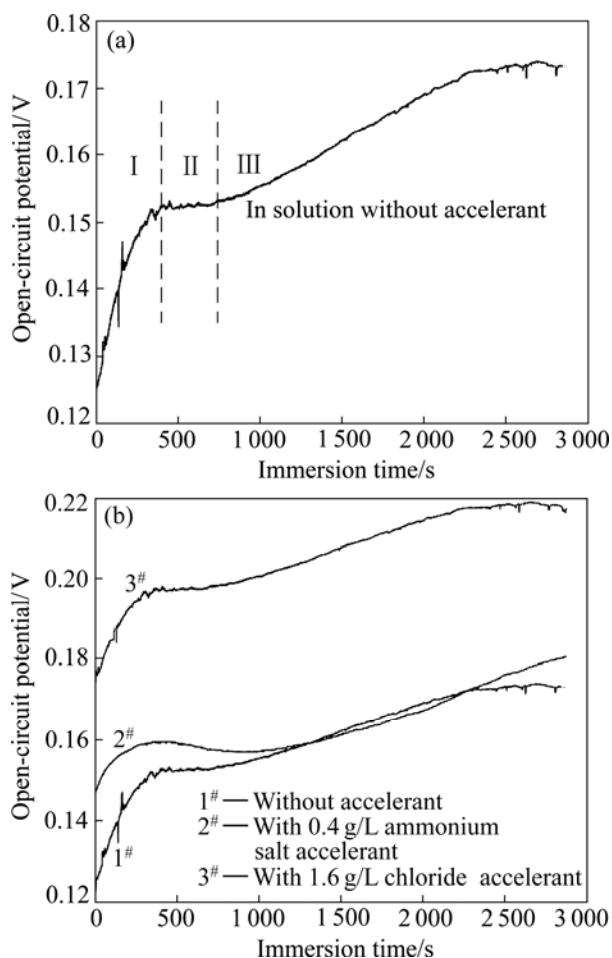

Fig.10 Potential change of Al specimen in coating growth process treated in different conditions

These two accelerants can shorten the time period in first stage from 6 to 5 min, accelerating the coating formation. Chloride will also shorten the time period of the second stage from 15 to 10 min, while accelerant of ammonium salt will prolong the duration in the second stage to 18 min. The prolonged time for the coating formation in the second stage will increase the coating thickness, but worsen the coating compactness. Therefore, compared with ammonium salt, chloride is more beneficial to the coating formation in the treating solution.

4 Conclusions

1) A good conversion coating on Al alloy surface can be prepared in the Ce(NO$_3$)$_3$ contained solution. The accelerant of chloride increases the coating compactness, and the ammonium salt increases the coating thickness, so these two accelerants can improve the coating corrosion resistance.

2) Accelerant of chloride increases the Ce content in the coating, while ammonium salt decreases the Ce content in the coating and leads to an increase in Al content, so they can facilitate the deposition of Ce or Al hydroxides. The valences of Ce element are +3 and +4. The coating, composed of metal oxide, metal hydroxide and hydrate, is in the amorphous structure.

3) The proposed scheme can describe the electrochemical reaction in the coating formation. The coating growth process can be divided into three stages. Chloride increases the initial potential of Al alloy and shortens the time period in the first and the second stage of coating formation.

References

[1]   ABDEL S H. Corrosion protection of aluminum composites by silicate/cerate conversion coating [J]. Surf Coatings Tech, 2006, 200(12/13): 3786−3792.

[2]   BIBBER J. Trivalent chrome conversion coating for zinc and zinc alloys [J]. Metal Finishing, 2007, 105(10): 425−435.

[3]   ABDEL S H. Advanced nano-particles anti-corrosion ceria based sol gel coatings for aluminum alloys [J]. Mater Lett, 2006, 60(21/22): 2633−2637.

[4]   NORDLIEN J H, WALMSLEY J C, ØTERBERG H, NISANCIOGLU K. Formation of a zirconium-titanium based conversion layer on AA 6060 aluminum [J]. Surf Coatings Tech, 2002, 153(1): 72−78.

[5]   BETHENCOURT M, BOTANA J, CANO M J, MARCOS M. High protective, environmental friendly and short-time developed conversion coatings for aluminum alloys [J]. Appl Surf Sci, 2002, 189(1/2): 162−173.

[6]   HUGHES A E, GORMAN J, HARVEY T G, MCCULLOCH D, TOH S K. SEM and RBS characterization of a cobalt-based conversion coating process on AA2024-T3 and AA7075-T6 [J]. Surf Interf Anal, 2004, 36(13): 1585−1591.

[7]   WILLIAM G F, O'KEEFE M J, ZHOU Hai-feng, GRANT J T. Characterization of cerium-based conversion coatings for corrosion protection of aluminum alloys [J]. Surf Coatings Tech, 2002, 155(2/3): 208−213.

[8]   ANDRÉ D, PETITJEAN J P. Study of the deposition of cerium oxide by conversion onto aluminum alloys [J]. Surf Coatings Tech, 2005, 194(1): 1−9.

[9]   CAMPESTRINI P, TERRYN H, HOVESTAD A, de WIT J H W.

Formation of a cerium-based conversion coating on AA2024: Relationship with the microstructure [J]. Surf Coatings Tech, 2004, 176(3): 365−381.

[10] GU Bao-shan, LIU Jian-hua. Corrosion inhibition mechanism of rare earth metal on LC4 A1 alloy with spilt cell technique [J]. J Rare Earths, 2006, 24(1): 89−96. (in Chinese)

[11] LI Ji, SUN Jie, AN Cheng-qiang. Research development of aluminium alloy with chromate-free passivation [J]. Surf Tech, 2008, 37(4): 60−62. (in Chinese)

[12] BETHENCOURT M, BOTANA F J, CANO M J, MARCOS M. Advanced generation of green conversion coatings for aluminum alloys [J]. Appl Surf Sci, 2004, 238(1/4): 278−281.

[13] LIU Yong-hui. Electrochemical determination technology [M].

Beijing: Aeronautic Institute of Beijing Press, 1987. (in Chinese)

[14] SHAO Min-hua, HUANG Ruo-shuang, FU Yan, LIN Chang-jian. Investigation of formation and inhibition mechanism of cerium conversion films on Al 2024 alloy [J]. J Rare Earths, 2002, 20(6): 640−645. (in Chinese)

[15] BÖHM S, GREEF R, MCMURRAY H N, POWELL S M, WORSLEY D A. Kinetic and mechanistic studies of rare earth-rich protective film formation using in situ ellipsometry [J]. J Electrochem Soc, 2000, 147(9): 3286−3293.

[16] CHEN Su, CHEN Xiao-fan, LIU Chuan-ye, ZHU Li, SUN Ji-qi. Rare earth conversion coatings of aluminum alloys [J]. Mat Prot, 2003, 8(36): 33−36. (in Chinese)

(Edited by YANG Bing)